Ultra Soft X-ray Absorption Spectroscopy and Photoelectron Spectroscopy Studies on Related Materials and Cathodes of Lithium Ion batteries

Hideshi ISHII[1], Koji NAKANISHI[1], Kazuo KOJIMA [2], Iwao WATANABE[1], and Toshiaki OHTA[1]

1) SR Center, Research Organization of Science and Engineering, Ritsumeikan University, 1-1-1 Noji-Higashi, Kusatsu, Shiga 525-8577, JAPAN

2) Department of Applied chemistry, College of Life Science, Ritsumeikan University, 1-1-1 Noji-Higashi, Kusatsu, Shiga 525-8577, JAPAN

Abstract

For analysis of lithium ion batteries, the ultra soft X-ray absorption spectroscopy beamline BL-2 at SR center of Ritsumeikan University has been improving: adding the new grating (900 l/mm) to the monochromator for higher energy up to 1000eV, and constructing the XAFS-PES (photoelectron spectroscopy) chamber equipped with in-situ transfer vessel systems. To elucidate the performance of this beamline, Li-K, O-K and TM-L XAFS and Li1s PES of related materials and cathodes have been measured. Finally, for precise analysis on the chemical state of Li, reference samples of Li compounds were also in-situ prepared by using deposition. Li K-XAFS spectra of deposited Li metal shows fine features compared with that of ground Li metal. A strong peak of Li1s photoelectron indicates that fresh surface layer of Li metal was prepared.

1. Introduction

For understating the mechanism of lithium ion batteries (LIB), it is one of the most important questions whether the electron comes from transition metal (TM) ion or oxygen ion when lithium ion leaves cathode of lithium ion battery. Electronic structures of TM3d and O2p reveals this answer. The electronic structures of late TM oxides, the grand state of the TM ions exists a mixed electronic state between $3d^n$ and $3d^n\underline{L}$ due to the M-O covalent character, where $\underline{L}$ means the oxygen ligand hole state by the charge transfer of O2p to TM3d [1,2]. Thus, soft X-ray absorption spectroscopy (XAS) of both TM L-edge and O K-edge is one of the most powerful tools because both TM2p→3d and O1s→2p transition are directly observed by using this method.

On the contrary, to answer complementary question, chemical state of Li ions during the charge-discharge cycles and where Li ions go, one can also measure Li K-edge X-ray absorption fine structure (XAFS). Photoelectron spectroscopy (PES) measurements of Li1s also give complementary information. Thus, for detailed analysis of lithium ion batteries, monochromatized X-rays with wide energy range from 50 to 1000 eV are needed.

The ultra soft-XAS beamline BL-2 at SR center of Ritsumeikan University consists of a conventional Monk-Gillieson monochromator, which was almost similar to that of BL-11[3] at this SR center. Therefore, the energy range of X-rays provided by 3 gratings of this BL-2 was almost same, 35-650 eV. For systematical analysis including late TM L-edge XAFS, such as Co and Ni L-edge, with enough energy resolution, another new grating is needed, which provides higher energy X-rays up to 1000eV. In addition, to avoid the change of chemical state of samples between preparation and measurement, *in-situ* sample introduction system into XAFS and/or PES measurement chambers without exposure to ambient air is also needed.

In this paper, we firstly present the outlines of this improved ultra soft XAS beamline BL-2 at SR center of Ritsumeikan University. Next, in order to elucidate the performance of this improved beamline, Li K-edge, O K-edge and TM L-edge XAFS and Li1s PES of related materials and cathodes measure at this beamline will be presented. Finally, we show Li K-edge XAFS of lithium reference samples prepared in-situ and elucidate their validities as more precise references for Li K-edge XAFS.

2. Improvements of the ultra soft X-ray absorption spectroscopy beamline BL-2

2.1. Improvement of the ultra soft XAS beamline

As mentioned above, we added the new grating (900 l/mm) to the monochromator for higher energy up to 1000 eV, and constructed both the XAFS-PES chamber and the

general-purpose XAFS chamber, equipped with *in-situ* transfer vessel systems. After these improvements, we found low frequency oscillations (0.2-10 Hz), *i.e.* rolling oscillations of gratings, which decrease energy resolution, in particular, in higher energy region. Setting a weight with the rotatable holder of gratings drastically suppressed these oscillations and achieved late TM L-edge XAFS measurements with high energy resolutions.

2.2. Outlines of the ultra soft XAS beamline

Figure 1 shows schematic diagram of this beamline. Photons which emit from source point go through with the acceptance angle of 5 mrad horizontally × 3 mrad vertically, by two-set apertures. Then, SR beam is pre-focused on entrance slit S1 horizontally and vertically by the spherical mirrors M1 and M2, respectively.

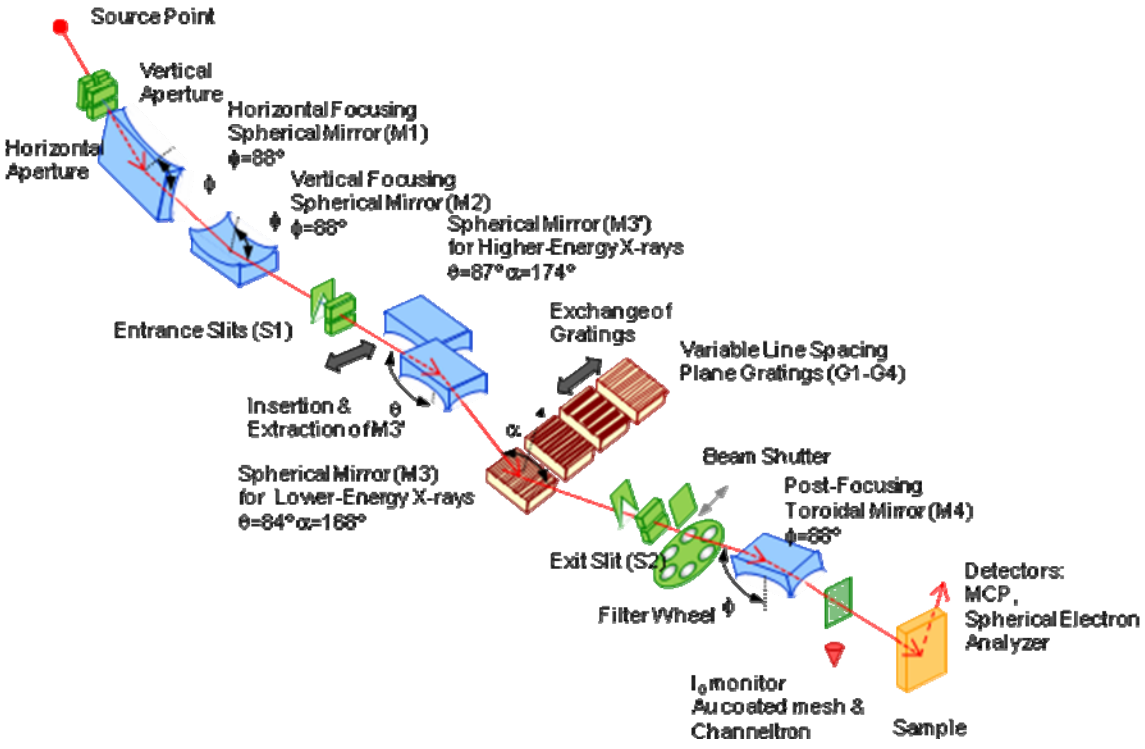

Fig. 1. Schematic diagram of ultra soft X-ray absorption beamline BL-2 at SR center of Ritsumeikan University.

After X-ray beam is focused vertically by spherical mirror M3 or M3', X-rays are monochromatized by a conventional Monk-Gillieson monochromator equipped with four varied-line-spacing (VLS) holographic plane gratings G1-G4; 300G (300 lines/mm), 1200G (1200 lines/mm), 600G (600 lines/mm) and newly installed 900G (900 lines/mm). These gratings are used interchangeably at an included angle of either 168° for lower energy X-rays or 174° for higher energy ones, by extracting or inserting of M3', respectively. Thus, one particular included angle and grating is easily selected without breaking vacuum. Although various combinations of these four gratings and two including angles make it possible to cover the wider energy range, we usually use 300G and 1200G for lower energy

XAS analysis below 350 eV, and 600G and 900G for higher energy region, respectively. The rotatable holder of gratings is newly equipped with two components: one is a weight to suppress the rolling oscillations and the other is the encoder to read present rotating angle of gratings. Monochromatized X-rays are vertically focused on the exit slit S2.

Finally by toroidal mirror M4, monochromatized X-rays are post-focused on the sample with the beam size of 0.6mm horizontally × 1.5mm vertically. Higher order diffractions are eliminated by using a proper filter set with filter whiles. Photon intensity of incident beam is monitored by the I_0 monitor between M4 and sample with two mode: measurement of leak current from gold mesh or detection of electrons emitted from same gold mesh by channeltron, where electrons are collected by high repulsive voltage around gold mesh.

As experimental chambers, we constructed two XAFS chambers. One is the general-purpose XAFS chamber, which equipped with microchannel plate (MCP) detector for total electron yield (TEY), partial electron yield (PEY) and total fluorescence X-ray yield (TFY) measurements. The other is the PES-XAFS chamber equipped with a spherical electron analyzer (R-SES-2002, VG Scienta) for PES measurements. Drain currents (sample currents) from samples can be also measured in both chambers as TEY measurements. Both chambers can be equipped with transfer vessel systems for *in-situ* sample introduction under inert ambient Ar or vacuum [4,5]. This system also realizes *in-situ* sample transportation between BL-2 and BL-10, which is a soft X-ray XAFS beamline with photon energy of 1000-4500eV.

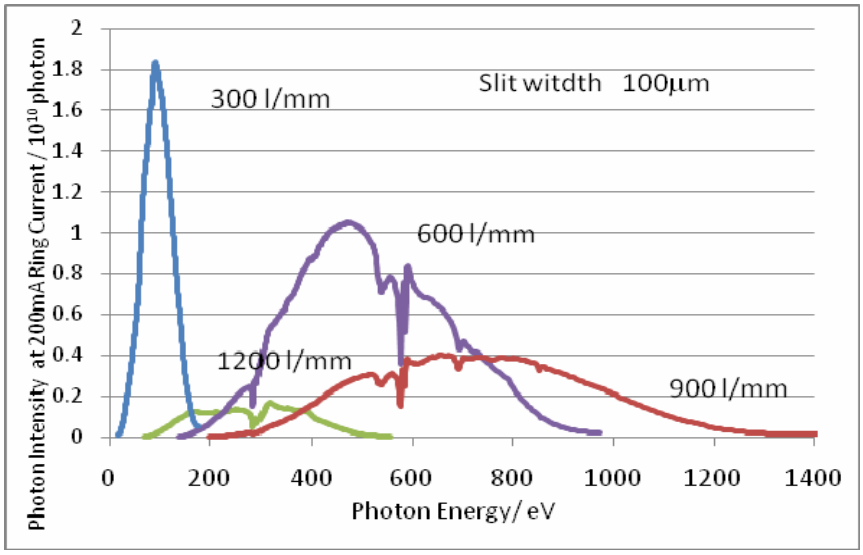

Fig. 2. Energy distributions of photon intensity of BL-2.

Figure 2 shows energy distribution of photon intensity of BL-2 by measuring sample currents (drain currents) of a clean gold plate. Slit width is fixed at 100μm for conventional XAFS measurements. Although absorption structures of optics (Cr L-edge) and contamination on optics (C K-edge) were observed, photon intensity of monochromatized

X-ray is about several $10^{10\text{-}9}$ photons. Higher order diffractions are also observed. As shown in Figure 2, at about 420 eV a small dip due to the Ni L_3-edge adsorption induced by 2nd order diffraction was observed. The ratio of 2nd order diffraction at 400 eV is roughly estimated about 5%. Thus it is considered that about several % of higher order diffraction still remains in monochromatized X-rays in all energy range. However some diffraction can be eliminated by selecting a particular filter.

.

3. XAFS and PES measurements of LIB cathodes and related materials

3.1. Experimental

In order to investigate the performances of improved BL-2, XAFS and PES of related materials of LIB and cathodes have been measured. After commercial grade $LiCoO_2$, CoO, Co_3O_4, NiO and $LiNiO_2$, were ground into fine powders, fine powders of related materials were dispersed over conductive carbon tape and mount on one sample holder. Cathodes were prepared by coating mixture of activate materials, carbon and polyvinylidene fluoride (PVdF) binder on thin Al foils. $LiCoO_2$ cathode (LCO), $LiMn_2O_4$ cathode (LMO) and two $Li(Ni_{1/3}Co_{1/3}Mn_{1/3})O_2$ cathodes (NCM) with different thickness were cut in the size of about 8mm×8mm and mounted on the other sample holder.

TEY and TFY XAFS spectra at same edge were simultaneously measured with normal incidence. TEY XAFS spectra were obtained by measuring sample currents. Fluorescence X-rays were collected by applying high negative voltage to a retarding grid in front of an MCP detector. While all electrons emitting form samples are repelled, all fluorescence X-rays including other fluorescence X-rays emit from other elements. Thus, we call “total” fluorescence X-ray yield (TFY). All spectra were normalized by intensity of incident beam I_0 using channeltron detection.

Li1s PES spectra of cathodes were measured at different excitation energy of 110 eV and 650 eV with pass energy of 200 eV. Photoelectrons were collected at normal emission geometry. Dwell time was 1s and the aperture of electron analyzer was used the straight shape aperture with the width 1.5 mm. Binding energy of Li1s was calibrated by assuming that of $Au4f_{7/2}$ peak from a chemically cleaned Au plate at 84 eV.

3.2. Results and discussion

Figure 3 shows XAFS spectra of related materials measured with a TEY mode. A new 900G grating and suppressing the rolling oscillations of gratings realized measurements of TM L-edge XAFS with enough high resolution to discuss the chemical state.

Obtained spectra are similar to those measured at previous works by O K- and TM L-XAFS [2,6-9]. A pre-edge peak at about 530 eV is assigned to the transition from O1s to

hybridized band between O2p and TM3d. As shown in Figure 3 (a), a sharp peak at 61.8 eV was observed in Li K-XAFS of $LiCoO_2$ while only broad peak exists in that of $LiNiO_2$ and similar to Li_2CO_3. In previous works of XAFS of $LiCoO_2$ [10] and electron energy loss near-edge structure (ELNES) of $LiNiO_2$ [11], a sharp peak at about 62 eV was observed. This sharp peak at 61.8 eV also exists in LiF and $LiPF_6$ and represents Li atom is more ionic. Li1s PES studies on $LiNiO_2$ [12] and $LiNi_{0.80}Co_{0.15}Al_{0.05}O_2$ [10] reveled Li_2CO_3 layer formed on surface of these particles. 200 keV electron as an ELNES probe with a long attenuation length can give bulk information while escape depth of Li1s photoelectron, which causes Li K-XAFS, is only 1-2 nm.

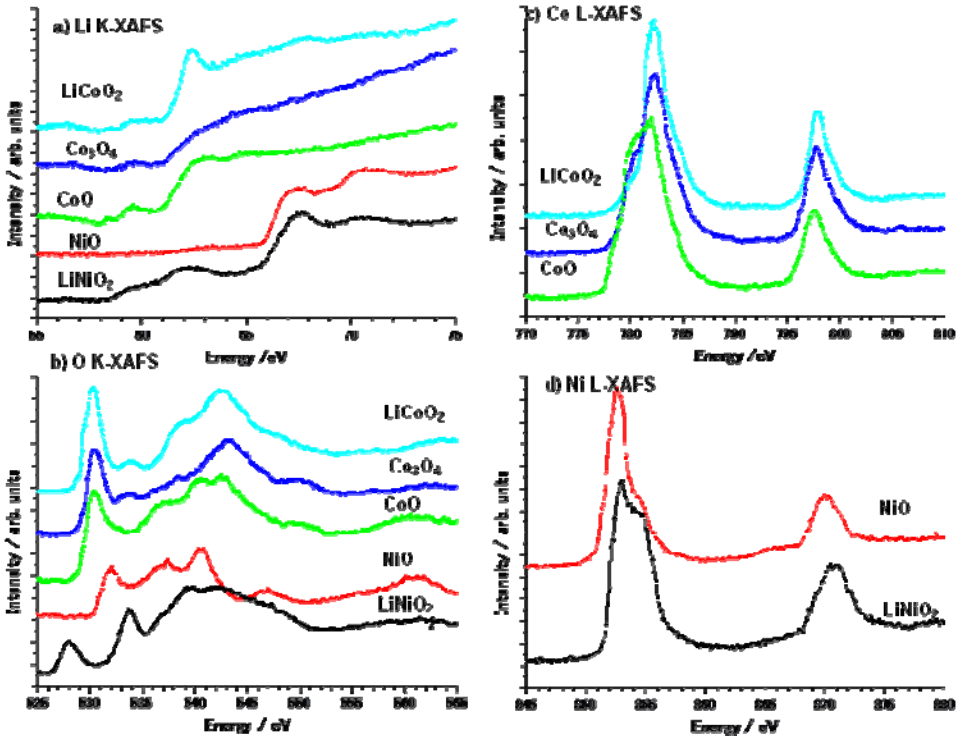

Fig. 3. TEY-XAFS spectra of LIB related materials; $LiCoO_2$, Co_3O_4, CoO, NiO, and $LiNiO_2$. a) Li K-XAFS (300G, slit width 100 μm), b) O K-XAFS (900G, slit width 100 μm), c) Co L-XAFS (900G, slit width 20 μm) and d) Ni L-XAFS (900G, slit width 20 μm), respectively

As well known, to investigate practical LIB cathodes, the difference between surface sensitive TEY and bulk sensitive TFY becomes more important. In particular, attenuation length of Li fluorescence X-ray is about 40 nm in typical cathodes [13]. Thus, using this difference, we can answer the question, “where does Li exist: solid-electrolyte interface (SEI) or bulk?” Li K-, O K- and Co L-XAFS spectra of cathodes measured with both TEY and TFY modes are summarized in Figure 4, 5 and 6, respectively.

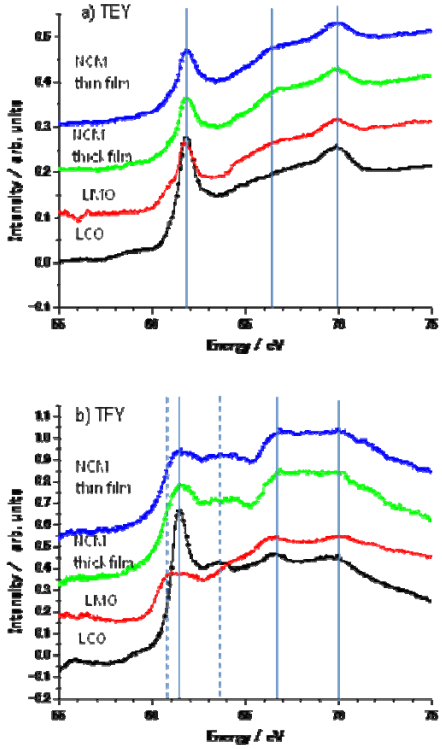

Fig. 4 Li K-XAFS of cathodes (300G, slit width 100 μm)

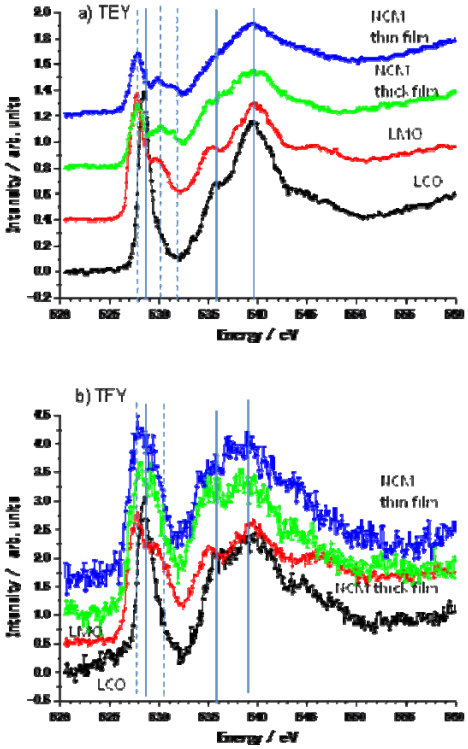

Fig. 5 O K-XAFS of cathodes (900G, slit width 50 μm)

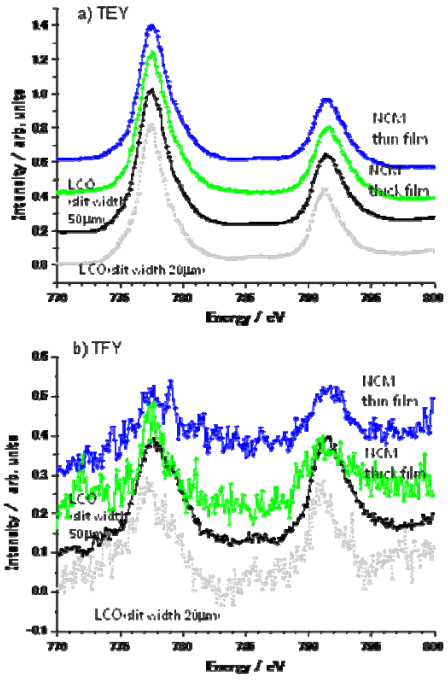

Fig. 6 Ni L-XAFS of cathodes (900G, slit width 50 μm)

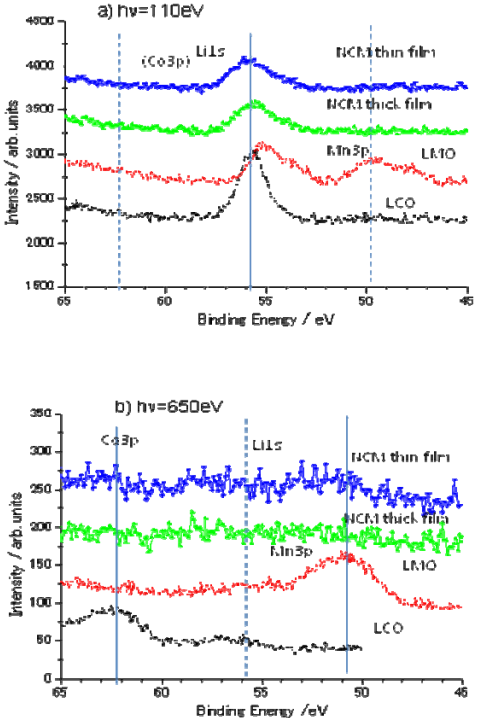

Fig. 7 Li1s PES of cathodes excited by a) 110 eV and b) 650 eV with pass energy of 200 eV

Li K-XAFS of LCO measured with TEY mode in Figure 4 is somewhat different from that of $LiCoO_2$ in Figure 3 (a): a peak at 61.8eV of LCO is sharper than activate material $LiCoO_2$ and similar to that of LiF. XAFS spectrum of LCO measured with TFY mode is rather different from TEY. This suggests Li in the surface layer of LCO is more ionic than bulk and activate materials. Similar trends are found in other cathodes. In particular, this peak of LMO measured with TFY mode shifts to rather lower energy and broadens. In TEY spectrum, small shift of main peak to lower energy and additional shoulder at about 61eV are observed.

On the contrary, O K-XAFS and Co L-XAFS of cathodes are almost similar except pre-edge peak in O K-XAFS. Compared with TFY detection of Li K-edge, lower S/B, which arises from no energy resolved detection using an MCP, makes spectra noisy ones. In addition, self- absorption effect distorts peaks and features in spectra. Thus, for the analysis of TM L-XAFS, we had better select the signal intensity (wide slit, such as 50 μm) rather than energy resolution (narrow slit, such as 20 μm) as shown in Figure 6.

Researches on chemical states of elements in LIB cathodes during charge-discharge cycles have been already performed at this beamline [14]. Furthermore, energy–resolved FY detection system using a large area silicon drift detector (SDD) is now developing for the more detailed analysis on O and TM.

Excitation energy dependence of Li1s PES measurement was summarized in Figure 7. At 110eV the ratio of photoionization cross section of Li1s to that of Co3p is about 2 while this ratio is about 1/16 at 650eV [15]. Thus, selecting excitation energy enables PES analysis focused on Li1s. Similar trend of Li1s from $LiCoO_2$ was already found [15], where Co3p was more intense compared with this study. One reason is the difference between a cathode and an activate material. The other reason is that their preparation with Ar sputtering might decrease Li on the surface because our Li1s PES measurement of $LiCoO_2$ also showed a weaker Co3p peak.

Li1s peak from LMO shifted to lower binding energy and had two components. This agrees with the behavior of XAFS spectra of LMO measured with TEY mode. Li1s PES spectra of other cathodes also agree with XAFS spectra measured with TEY mode.

4. XAFS and PES measurements of *in-situ* prepared Li references

As mentioned above, chemical state of Li is easily changed by various causes. Preparation of reference samples may affect results. Finally, we demonstrated *in-situ* preparation of various Li references for more precise analysis on chemical states of Li.

Figure 8 shows Li K-XAFS of Li metals prepared with different methods. In spite of *in-situ* introduction using an Ar-filled glove box and the transfer vessel, obtained XAFS spectra indicated that surface changed Li_2CO_3 and interfacial layers like Li_2O grew. Next Li metal surface was grounded by a file and/or sand paper to eliminate surface layer. TEY XAFS spectra of this ground Li metal indicates that the contribution of Li_2CO_3 decreased. Bulk-sensitive TFY measurement revealed a step at about 58 eV and a peak at 63 eV, which were also observed in previous work [17, 18]. Using an Ar-filled glove box and a conventional one, a deposition system by heating a W-filament was in-situ constructed and equipped with the XAFS-PES chamber. While a piece of Li metal mentioned above was used as deposition source and Li metal was deposited on In plate under the vacuum of 10^{-5} Torr, measured TEY XAFS spectrum shows fine features compared with TFY XAFS spectrum of ground Li metal and those measured in previous works. Although deposition on In plate may induce the reaction between In and Li at the interface, Li K-XAFS spectrum of this surface indicates thick Li metal layer grew.

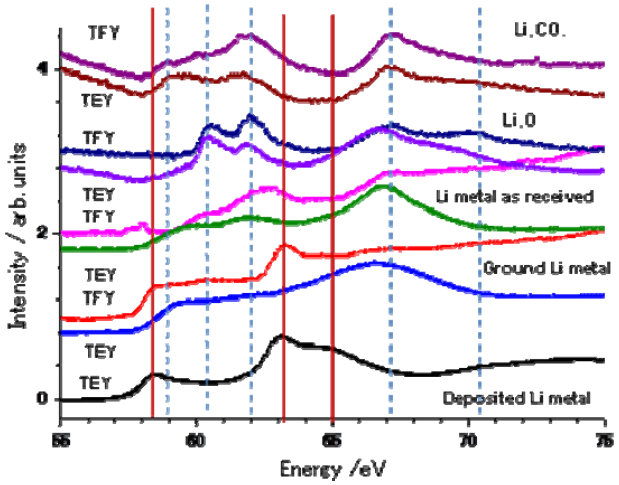

Fig. 8. Li K-XAFS of Li metals prepared with different methods.

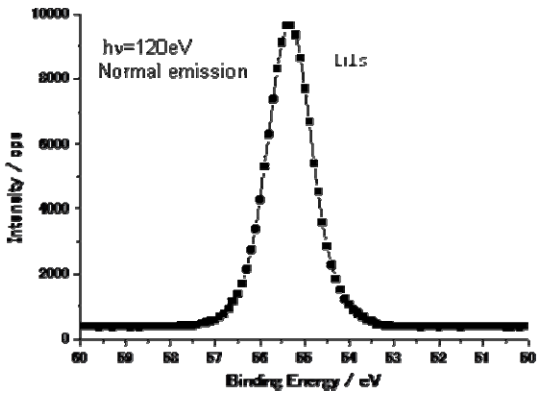

Fig. 9 Li1s PES of deposited Li metal.

To confirm the chemical state of this deposited surface, Li1s PES spectra were measured. Figure 9 shows Li1s PES excited by 120 eV with the pass energy of 50 eV and 0.5 mm width curved aperture. Lower background and a strong peak also suggest the growth of Li metal thick layer.

5. Conclusions

For more precise analysis on LIB, improvements of ultra soft XAS beamline have been performed and realized measurements of Li K-, O K-, and TM L-XAFS and PES at the same beamline, with *in-situ* sample introduction and *in-situ* reference preparation. Although there remains some problems, such as small rolling oscillations of grating, high order diffractions, and lower S/B TFY detection using an MCP detector, further improvements being performed now solve these problem and lead us to further practical analysis on the mechanism of LIB.

Acknowledgement

Part of this work was supported by Research and Development Initiative for Scientific Innovation of New Generation Batteries (RISING) project from New Energy and Industrial Technology Development Organization (NEDO) in Japan. We greatly acknowledge it. We thank to Dr. Masato MOGI and Prof. Yoshiharu UCHIMOTO (Kyoto Univ. and RISING project) for their preparation of cathode samples measured in this study. We also thank to Prof. Sigero IKEDA (SR center, Ritsumeikan Univ.) for his stimulating discussion and kindness advice.

References

[1] J. Zaanen, G. A. Sawatzky and J. W. Allen, Phys. Rev. Lett. **55**, 418 (1998).,

[2] F. M. F. de Groot, M. Grioni, J. C. Fuggle, J. Ghijsen, G. A. Sawatzky and H. Petersen, Phys. Rev. **B 40**, 5715 (1989).

[3] M. Koike et al., Rev. Sci. Instrum. **73**, 1541 (2002).

[4] K. Nakanishi, S. Yagi and T. Ohta, IEEJ Trans. EIS **130**, 1762 (2010) (in Japanese).

[5] K. Nakanishi et al.,AIP Conf. Proc. **1234**, 931 (2010).

[6] J. van Elp, J. L/ Wieland, H. Eskes, P. Kuiper, G. A. Sawatzky, F. M. F. de Groot and T. S. Tunner, Phys. Rev. **B 44**, 6090 (1991).

[7] C.-H. Chen, B.-J. Hwang, C.-Y. Chen, S.-K. Hu, J.-M. Chen, H.-S. Sheu, J.-F. Lee, J. Power Sources **174**, 938 (2007).

[8] V. R. Galakhov, M. Neumann and D. G. Kellerman, Appl Phys **A 94**, 497 (2009).

[9] Y. Uchimoto, H. Sawada and T. Yao, J. Power Sources **97-98**, 326 (2001).
[10] H. Kobayshi, S. Emura, Y. Arachi and K. Tatsumi, J. Power Sources **174**, 774 (2007).
[11] Y. Koyama, T. Mizoguchi, H. Ikeno and I. Tanaka, J. Phys. Chem.. B 109, 10749 (2005).
[12] A. W. Moses, H. G. Garcia Flores, J.-G. Kim and M. A. Langell, Appl. Surf. Sci. **253**, 4782 (2007).
[13] B.L. Henke, et al., Atom. Data and Nucl. Data Tables **54**, 181 (1993).
http://henke.lbl.gov/optical_constants/
[14] M. Oishi et al,, to be published.
[15] J.J. Yeh and I.Lindau, Atomic Data and Nuclear Data Tables, **32**, 1 (1985).
[16] K. Maeda,et al.,, Adv. X-ray Chem . Anal., Jpn. 35, 137 (2004) (in Japanese).
[17] J. Tsuji, H. Nakamatsu, T. Mukoyama, K. Kojima, S. Ikeda and K. Taniguchi, X-ray Spectrom. 31319 (2002).
[18] A. Braun, H. Wang, J. Shim, S. S. Lee and E. J. Cains, J. Power Sources **170**, 173 (2007).